

## Review Article

# A Comprehensive Review of Thermal Barrier Coatings Microstructure with Different Platinum-Modified Aluminide Bond Coats

A. Rabieifar\*

Advanced Materials Engineering Research Center, Karaj Branch, Islamic Azad University, Karaj, Iran

Received: 03 January 2023 - Accepted: 08 June 2023

## Abstract

Thermal Barrier Coatings (TBCs) are used to protect the surface of hot components of gas turbines. TBCs usually have three layers and include a Top Coat (TC) ceramic layer, an intermediate metallic Bond Coat (BC) layer, and a Thermally Grown Oxide (TGO) layer. In the present study, a brief survey of the microstructure of the ceramic layer produced by Air Plasma Spray (APS) and Electron Beam Physical Vapor Deposition (EB-PVD) has been done. Due to the inherent microstructure of the top coat ceramic layer, Diffusion aluminide bond coats are widely used in thermal barrier coatings for oxidation and hot corrosion resistance of Ni-base superalloy components of advanced gas turbine engines. Modifying these coatings by Pt addition considerably improves their high-temperature oxidation resistance. This effect of Pt has prompted intense research on the microstructure and oxidation behavior of Pt-modified aluminide coatings (Pt-Al) over the past several decades. The present review is to collate the available information on the subject. The study includes traditional  $\beta$ -(Ni, Pt)Al bond coats as well as the Pt-modified  $\gamma$ - $\gamma'$  type of bond coats that have gained prominence in more recent times. A brief description of typical process steps involved in the formation of Pt-aluminide coatings is provided followed by a detailed assessment of coating microstructures reported under various processing conditions. The influence of prior diffusion treatment, on the coating microstructure, is highlighted. The various mechanisms of the role of Pt in enhancing the oxidation and resistance of aluminide coatings, as suggested in the literature, are discussed.

**Keywords:** Pt-Aluminide Bond Coat, Diffusion Coating, Thermal Barrier Coating, Air Plasma Spray, Ni-Based Superalloy.

## 1. Introduction

High-temperature gas turbines of aero-engines are exposed to degradation mechanisms in their service environment. These mechanisms include creep, fatigue, oxidation, and hot corrosion.

Damages of hot components of gas turbines include internal degradations and surface degradations. Internal degradations are often obtained under high-temperature stresses, including the coarsening of  $\gamma'$ -Ni<sub>3</sub>(Al, Ti) precipitates, deformation and transformation of MC carbides, and the formation of creep cavities. Surface degradations include creep deflection, low and high-cycle thermal fatigue, wear fretting, hot corrosion, isothermal and cyclic oxidation, and foreign object damage [1-5].

A schematic of a gas turbine is shown in Fig. 1. A gas turbine of a jet engine is a rotating machine that works based on the energy of combustion gases. Each gas turbine consists of a compressor to compress the air, a combustion chamber to mix the air with the fuel and ignite it, and a turbine to convert the energy of the hot gases into the driving force to rotate the turbine. Air enters the turbine compressor from one side and is compressed before fuel is added.

The air passes through several rows of vanes and blades along the turbine shaft. In the combustion chamber, compressed air is mixed with fuel. Then the hot air causes the rotation of the turbine blades, and finally, the exhaust gases of the turbine come out [6]. The fuel used in these turbines is usually natural gas or petroleum products. Petroleum products often contain nitrogen, carbon, and vanadium (as the main fuel impurity) compounds, oxide, sulfide, and disulfide compounds, and depending on the service environment, alkali metals salt [6]. In gas turbines, the average temperature of the blades is about 950 °C. But the temperature can increase to more than 1100 °C. In some cases, the inlet temperature of the turbine increases up to 1650 °C. This temperature is higher than the melting temperature of the materials from which the blades are made. Therefore, cooling systems and heat-resistant coatings are needed to protect the turbine blades from oxidation and hot corrosion [8]. Fig. 2. shows the cross-section of a jet engine with a protective coating. As can be seen, the protective coating system is used in the high-pressure components of the turbine. Application of TBCs enables increasing engine performance by either increasing the turbine inlet temperature or reducing the cooling air flow. Alternatively the lifetime of the turbine blades can be extended by decreasing metal temperatures [9].

\*Corresponding author

Email address: a.rabieifar@kiaou.ac.ir

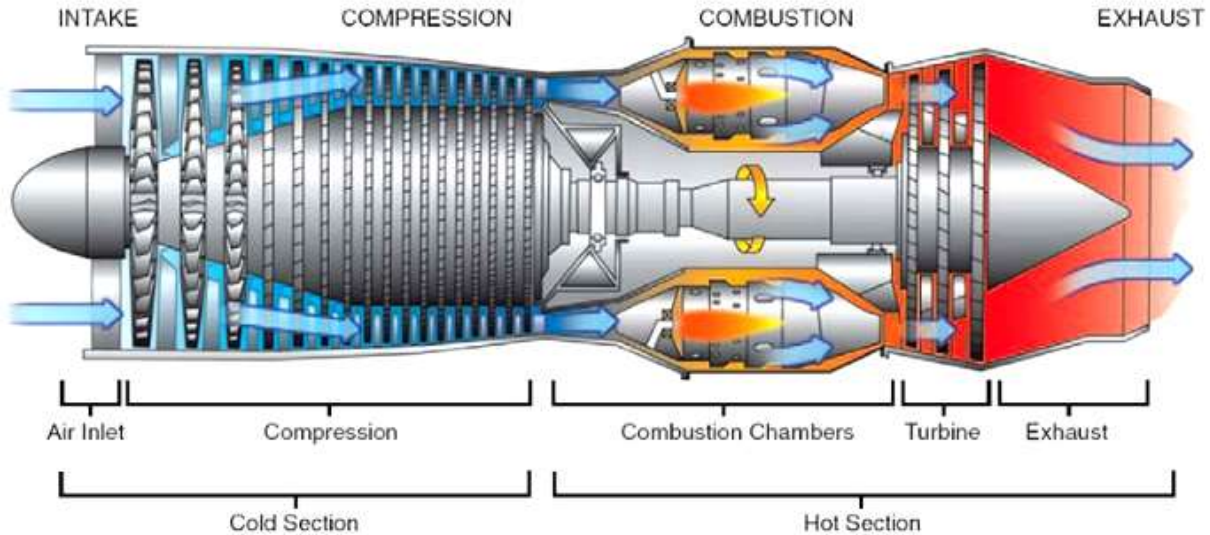


Fig. 1. A section of a typical gas turbine engine [7].

Thermal barrier coatings create thermal insulation at the components/atmosphere interface and reduce the component's surface temperature. TBCs with a thickness of up to 200  $\mu\text{m}$  can reduce the surface temperature of the superalloy substrate up to 180  $^{\circ}\text{C}$  [10-12]. The most important features of these coatings consist of corrosion and oxidation resistance, erosion resistance, the ability to create a metallurgical bond with the substrate, low thermal conductivity, uniform thickness, and sufficient flexibility against substrate deformation [13].

## 2. Thermal Barrier Coatings

The thermal barrier coatings consist of two ceramic layers and two metallic layers, which have different physical, thermal, and mechanical properties. These four layers are, from top to bottom, ceramic top coat, thermally grown oxide (TGO) (due to the bond coat oxidation during service condition), high aluminum concentration bond coat, and superalloy substrate. A schematic of a thermal barrier coating system is shown in Fig. 3.

### 2.1. Ceramic Top Coat

The commonly used TBC material 6–8 wt.% yttria-stabilized zirconia (YSZ), which performs quite well up to 1200  $^{\circ}\text{C}$  because of its high melting point (2700  $^{\circ}\text{C}$ ), low thermal conductivity (2  $\text{W m}^{-1} \text{K}^{-1}$ ), high coefficient of thermal expansion (CTE,  $11 \times 10^{-6} \text{K}^{-1}$ ), and low density (6.4  $\text{g/cm}^3$ ). Also, some other YSZ properties consist of low chemical reaction with the TGO layer (made of alumina), wear resistance and phase stability at temperatures below 1200  $^{\circ}\text{C}$  [14], high Young's modulus at ambient temperature (240 GPa), Good adhesion to the substrate, chemical inertness, low sintering rate and porous structure up to about 15%, which is essential for high strain compliance and

reduced thermal conductivity [13, 15-18]. These coatings are deposited in two ways - APS and EB-PVD [19]. In the EB-PVD method, the microstructure of the ceramic coating is columnar and has a higher strain tolerance than the APS method, which has a layered structure. On the other hand, the deposition cost of APS coatings is lower and due to the presence of micro-voids and micro-cracks, it has a lower relative thermal conductivity compared to EB-PVD coatings [20, 21]. APS coatings have a thermal conductivity in the range of 0.8-1  $\text{Wm}^{-1} \text{k}^{-1}$  at 25  $^{\circ}\text{C}$ , which is much lower than that of EB-PVD coatings at the same temperature [22]. Therefore, APS coatings have better thermal protection but less resistance to spallation compared to EB-PVD coatings. In the APS process, ceramic powder with a particle size of lower than 10  $\mu\text{m}$  is injected into an arc plasma jet and deposited onto the substrates. Within the plasma jet, the particles are accelerated and melted, followed by impaction, rapid solidification, and forming a coating on the substrate [20, 21]. The uniform plasma spraying parameters consist of flow rate of primary gas (plasma gas: Ar/H<sub>2</sub>), flow rate of carrier gas (Lit/Min), feedstock giving rate (g/min), spray distance (mm), spray angle (Deg), current (A) and arc voltage (V) [24]. All the mentioned variables affect the microstructure and properties of TBC coatings, their adhesion, and porosity. By increasing primary gas flow, inter-layer separation and micro-porosities decrease, but thermal conductivity increases [25]. In APS process, powder particles have high thermal energy and low kinetic energy. This feature reduces the plastic deformation of particles and creates porous coatings. The porosities provide short-circuit paths for the permeation of oxygen anions. As a result, the oxidation continues and the TGO layer at the BC/TC interface becomes thicker [26].

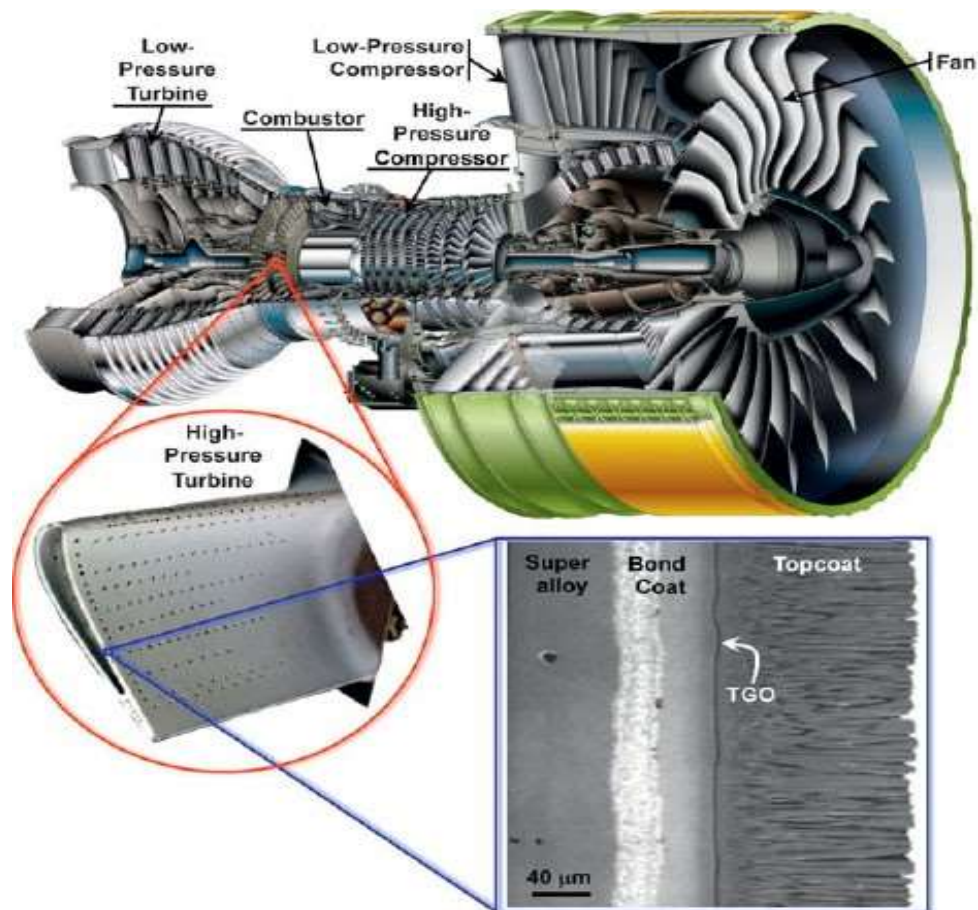


Fig. 2. A photograph of a turbine blade (~10 cm long) with thermal-barrier coating (TBC) from the high-pressure hot section of an engine, and a scanning electron microscope (SEM) image of a cross-section of an electron beam physical vapor deposited 7 wt% yttria-stabilized zirconia TBC [13].

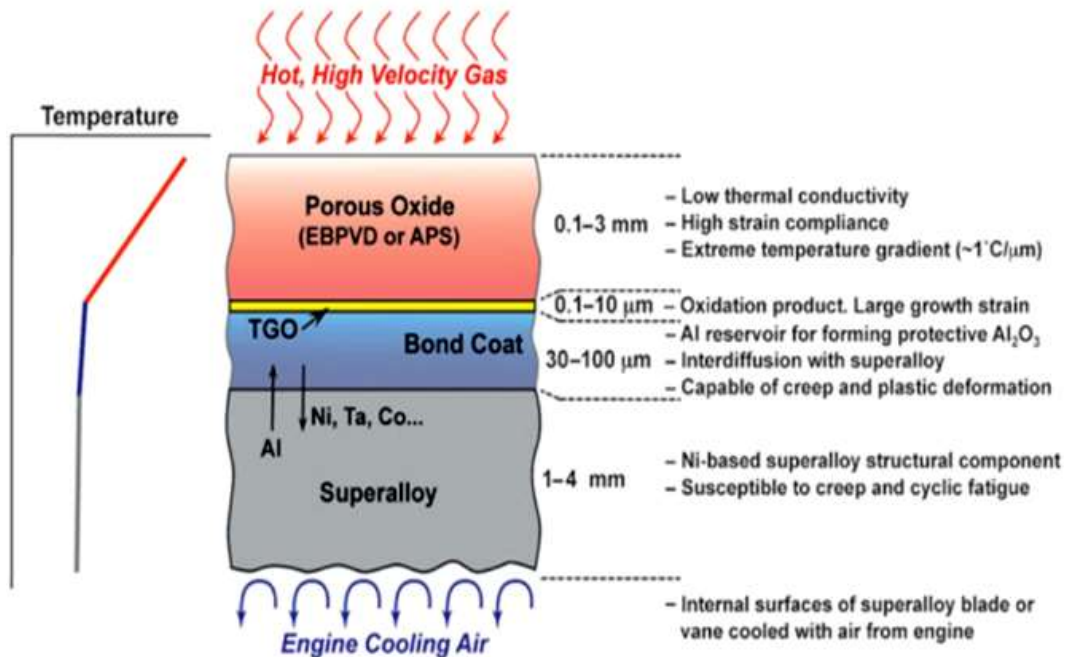


Fig. 3. A Schematic illustration of the multilayer, multi-functional nature of the thermal barrier coating system. The ceramic top coat is deposited by electron beam physical vapor deposition (EBPVD) or air plasma-spraying (APS). Sandwiched between the top coat and the metallic bond coat is the thermally grown oxide (TGO). Properties/functions and approximate thicknesses of the different layers are indicated [23].

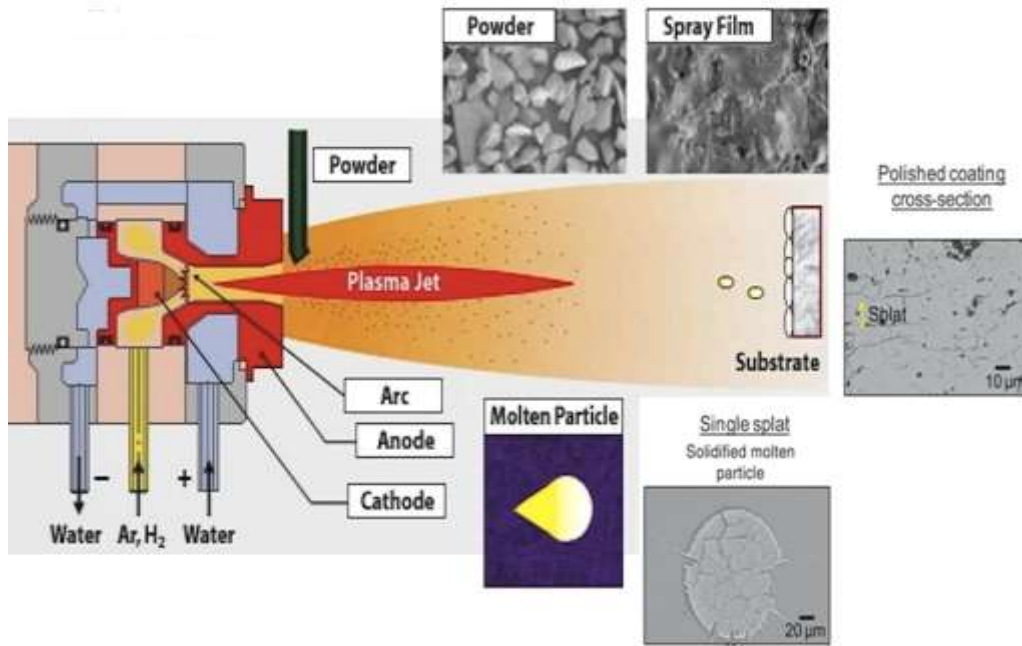


Fig. 4. A schematic illustration of the formation of the YSZ coating produced by the APS method [29].

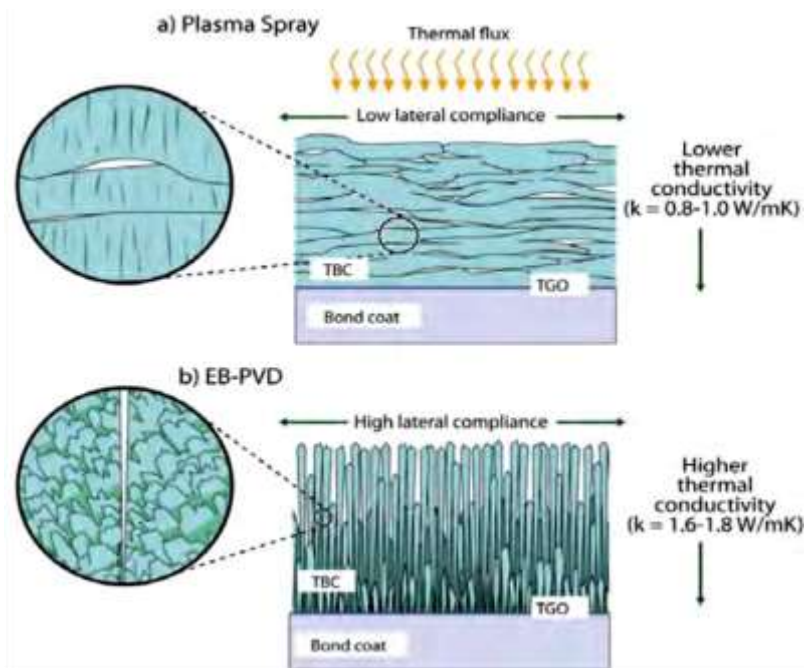


Fig. 5. A Schematic of porosities in a) YSZ APS coating, b) YSZ EB-PVD coating. In the APS YSZ coating, the large porosities are parallel to the substrate surface, creating inter-splat cracks. In the YSZ EB-PVD coating, the elongated porosities are perpendicular to the substrate surface, creating the inter-columnar gaps [22].

Liu et al. [27] found that in APS coatings if the sprayed spherical particles, undergo plastic deformation, and are placed on top of each other as flake particles, sintering occurs. APS coatings have a layered structure. These layers are composed of frozen droplets (splat). Research has shown that micro-porosities and micro-cracks cause non-linear elastic stress-strain behavior of the APS coating [28].

A schematic illustration of the formation of the YSZ coating produced by the APS method is shown in Fig. 4. The YSZ coating contains internal micro-cracks of the splats. Micro-cracks are created due to the relaxation of tensile stresses during splat solidification on the substrate [30]. Fig. 5. shows the difference between the EB-PVD YSZ and APS-YSZ microstructures in terms of the porosity difference in the coating.

The porosities are located perpendicular to the temperature gradient direction of the coating and on the boundaries of the splats. Micro-porosities affect reducing thermal conductivity [31].

The layered microstructure of ceramic coatings applied by the APS method is shown in Fig. 6. As can be seen, these coatings are porous, and oxide impurities and micro-porosities are located in the inter-splats spaces. Micro-porosities provide short-circuit for oxygen and corrosive materials to penetrate through the ceramic coating layer [12]. The main problem with using these coatings is the spallation of the ceramic top coat due to the thermal stresses produced during thermal cycles. Thermal stresses are generated due to the mismatch of the thermal expansion coefficients of the bond coat and top coat [32, 33]. APS coatings reduce the temperature of the substrate and increase its useful life. This issue leads to an increase in the inlet temperature and the efficiency of the turbine engine. In addition to reducing thermal expansion mismatch stresses, TBCs must also withstand severe thermal gradients [11].

## 2.2. Metallic Bond Coat

The bond coat protects the substrates from oxidation and improves the adhesion of the ceramic top coat to the metallic substrate. In addition, due to their porous nature, ceramic top coats are permeable to the corrosive compounds of the gas turbines' atmosphere [34]. Therefore, bond coats are needed to protect the substrate against degradation surface phenomena such as hot corrosion and oxidation. Bond coats generally have surface roughness and have proper adhesion to the ceramic top coat and the substrate [10]. Bond coats are often metallic and are more hot corrosion-resistant than the substrate. Bond coats (with a thickness of up to 100  $\mu\text{m}$ ) include aluminide diffusion coatings (modified with Pt, Cr, Si), MCrAlY (M= Ni, Cr) overlay coatings, and slurry coatings [11, 19, 35]. The chemical composition of the bond coat is designed so that during service conditions, a thin continuous layer usually made of  $\alpha\text{-Al}_2\text{O}_3$  (with a thickness of less than 1  $\mu\text{m}$ ) called the TGO layer is formed at the BC/TC interface, which prevents the downward diffusion of gases and corrosive salts to the substrate. The most important features of the TGO layer are chemical stability, slow growth, high density, and sufficient adhesion to the bond coat. In the service conditions of gas turbines, only oxides such as  $\text{Al}_2\text{O}_3$ ,  $\text{Cr}_2\text{O}_3$ , and  $\text{SiO}_2$  have the mentioned characteristics. But nowadays, because the protective layers of  $\text{Cr}_2\text{O}_3$  and  $\text{SiO}_2$  turn into  $\text{SiO}$  and  $\text{CrO}_3$  volatile oxides at temperatures over 1000  $^\circ\text{C}$ , bond coats with the ability to form  $\text{Al}_2\text{O}_3$  are used generally. Besides,  $\text{Al}_2\text{O}_3$  has a more suitable application in coatings designed for high temperatures due to its slower growth rate than other oxides.  $\text{Al}_2\text{O}_3/\text{YSZ}$  lamella

composite coatings have also been used as a ceramic top coat on the bond coats. Keyvani et al. [36], Afrasiabi et al. [12], and Chen et al. [37] determined that the crucial factor in the hot corrosion resistance of the nickel-based superalloy substrate in a corrosive environment containing  $\text{Na}_2\text{SO}_4 + \text{V}_2\text{O}_5$  molten salt caused by alumina (TGO) formation on the surface of the bond coat and prevent YSZ spallation. Diffusion coatings should have high density and thermodynamic stability [39].

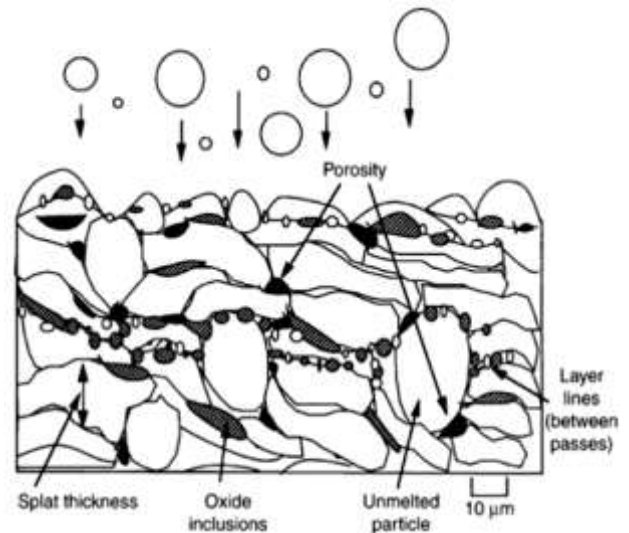


**Fig. 6. Cross-section of an atmospheric plasma sprayed coating showing common features [38].**

These coatings should serve as the principal source of TGO protective layer formation and a barrier against the diffusion of other elements from the substrate to the coating. Because the upward diffusion of the substrate elements into the coating weakens the mechanical properties of the coating and reduces the hot corrosion resistance and adhesion at the TGO/BC interface [23]. The addition of elements such as Hf and Y leads to a reduction in the rumpling of the BC/TGO interface and a reduction in TBC spallation [40]. Aluminide coatings are subject to extensive degradation at 600-850  $^\circ\text{C}$  and temperatures above 1050  $^\circ\text{C}$ . In the temperature range of 600-850  $^\circ\text{C}$ , the presence of sulfur and vanadium compounds causes high-temperature hot corrosion in the coating. The corrosion rate depends on variables such as the chemical composition of the coat, the concentration of corrosive compounds on the surface, and the duration of hot corrosion. In the temperature range of 900-1000  $^\circ\text{C}$ , due to the protection of  $\text{Al}_2\text{O}_3$  and  $\text{Cr}_2\text{O}_3$  oxides, oxidation continues at a lower rate. At temperatures over 1000  $^\circ\text{C}$ , the oxidation rate of the coat increases, and the inter-diffusion of coating and the substrate accelerates. As a result, the amount of aluminum and chromium in the coat decreases significantly, and the oxidation rate of the coating increases [41].

### 3. Plain Diffusion Aluminide Coatings

Diffusion coatings are often applied to produce the  $\beta$ -NiAl phase. This phase protects the metallic substrate by producing an  $\text{Al}_2\text{O}_3$  TGO layer. In the powder pack cementation method, components to be aluminized are embedded into a mixture of the aluminum source, an inert matrix (typically alumina sand), and a halide salt activator (e.g.,  $\text{AlF}_3$  or  $\text{NH}_4\text{F}$ ). The aluminum sources can be aluminum or aluminum-containing alloys, such as CrAl, CoAl, or NiAl. Alloy donors are used to increase the donor melting temperature and define the chemical activity of aluminum, allowing the coating microstructures to be tuned for improved performance. The pack is located in a retort and heated to temperatures in the range 650-1200 °C in a non-oxidizing atmosphere, such as argon or hydrogen. On heating, the halide activator transports aluminum from the donor to the surface of the target component, where it decomposes, releasing aluminum to diffuse into the alloy and cycling the halide back to the donor to pick up more aluminum [23]. This method is done with two types of processes:

**Low Activity High Temperature (LAHT):**

At temperatures above  $\sim 1050$  °C and with packs having low-aluminum activity donors,  $\beta$ -NiAl coatings form via predominantly outward diffusion of the nickel from the substrate. The  $\beta$ -NiAl phase contains a limited amount of refractory elements of the substrate. These coatings are typically single-phase and have Al: Ni ratios less than unity.

**High Activity Low Temperature (HALT):**

At temperatures below  $\sim 1000$  °C, and especially when the packs have high-activity donors (e.g., metallic aluminum), coatings grow by predominantly inward diffusion of aluminum. Then, during an annealing heat treatment, the  $\delta$ - $\text{Ni}_2\text{Al}_3$  phase turns into the  $\beta$ -NiAl. In this process, the refractory substrate elements such as tungsten, molybdenum, and tantalum are present in the coating as a substitutional solid solution or secondary phase precipitates in the outer parts of the coat. In the LAHT process, there are no Kirkendall pores in the coating, and due to the diffusion of nickel from the substrate, the coat forms outwardly. In the HALT process, diffusion of aluminum from the coat to the substrate occurs, and Kirkendall Pores are usually obtained in the coating [42-44]. The cross-section of LAHT and HALT aluminide coatings after heat treatment are shown in Fig. 7. As can be seen, after heat treatment, the HALT coating has two layers and an Inter-diffusion Zone (IDZ). The outer layer consists of an aluminum-rich  $\beta$ -NiAl matrix phase with substrate elements and dispersed carbides with the

chemical composition of  $\text{M}_{23}\text{C}_6$ ,  $\text{M}_6\text{C}$ , and MC. The inner layer contains a  $\beta$ -NiAl matrix phase rich in aluminum and without substrate elements and carbide precipitates.

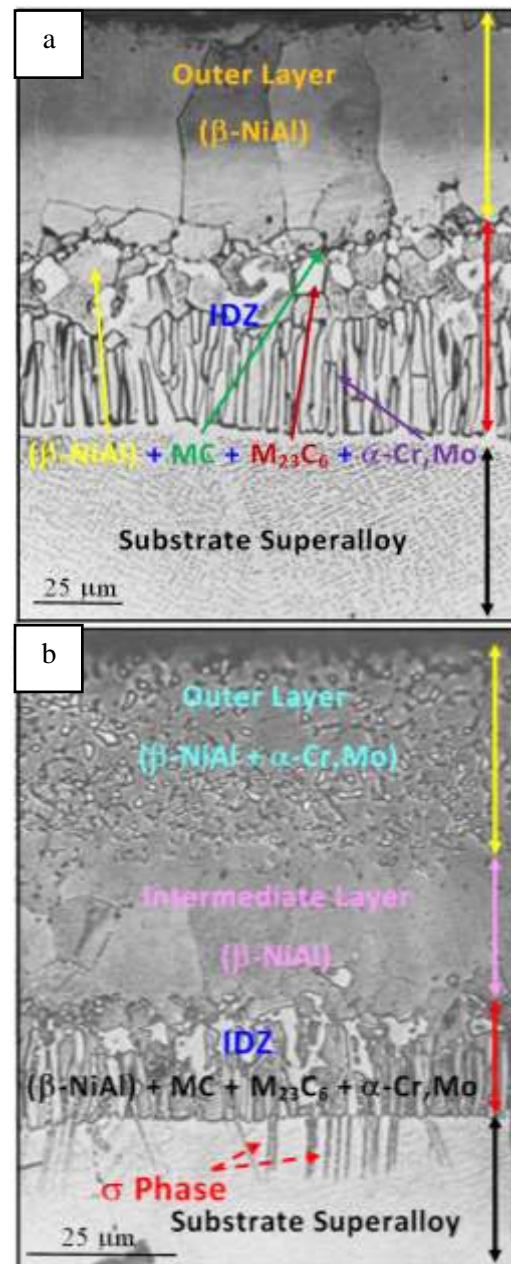


**Fig. 7. Typical microstructures of plain aluminide coatings: (a) outward-grown or LAHT, and (b) inward-grown or HALT. The various coating layers have been marked [53].**

The IDZ consists of metal carbides of refractory substrate elements such as tantalum, molybdenum, and tungsten or complex intermetallic phases in the NiAl or  $\text{Ni}_3\text{Al}$  matrix. The formation of these phases is often caused by the upward diffusion of nickel from the substrate [45]. LAHT coatings consist of two layers. These layers are the same as the two layers of HALT coatings [46].

Repeated spallation of aluminide coating during thermal cycles leads to rapid aluminum depletion from the coat and reduction of oxidation resistance. For solving this problem, elements such as silicon, chromium, zinc, and platinum have been placed at Ni atoms sites in the  $\beta$ -NiAl crystal structure substitutionally [47-52]. Lehnert and Meinhard [54] produced the first commercial Pt-Al coating system named LDC2. The outer layer of this coating consisted of a  $PtAl_2$  phase containing nickel. A second commercial Pt-Al coating named RT-22 was produced using the same process as the LDC2 coating. The outer layer of this coating consisted of a  $PtAl_2$  phase in the form of dispersed particles in the  $\beta$ -NiAl matrix. One of the sources of Al in Pt-Al coatings is the  $PtAl_2$  phase. On the other hand, this phase leads to brittleness in the BC/TBC interface. If the Pt-Al coating is used only to protect the turbine blades against oxidation and hot corrosion, the presence of  $PtAl_2$  will be beneficial. But if the coating is used as a bond coat, the  $PtAl_2$  phase will transform to the  $\beta$ -(Ni,Pt)Al phase at high-temperature service conditions. The above transformation leads to the production of tensile stress in the coating. This event degrades the TGO/YSZ interface and reduces the lifespan of TBC [52].

The Pt-Al coatings are usually formed in 4 distinct steps. Initially, a pure platinum layer with a thickness of 5-10  $\mu\text{m}$  is deposited on the superalloy substrate. Electroplating technique is most widely used for Pt deposition, although other methods such as physical vapor deposition (PVD) and fused salt electrolysis [55, 56] have also been adopted for this purpose.

#### 4. Diffusion Pt-Aluminide Coatings

In the second step, the plated substrate is given a diffusion heat treatment in vacuum, which is also termed as "prior diffusion" or "pre-aluminizing diffusion" treatment, for improving the adhesion of the plated layer with the substrate. This treatment also causes certain amount of inter-diffusion between the substrate alloy and the Pt layer. In the third step, the diffusion-treated substrate is aluminized to introduce Al for coating formation. Finally, a suitable post aluminizing heat treatment is given to the coated substrate at  $\sim 1070$   $^{\circ}\text{C}$  for completing the formation of the coating. This treatment also helps the substrate alloy regain the loss in mechanical properties, if any, caused by the high temperature exposure during the various coating steps [52]. Except for powder pack cementation, other aluminizing methods such as out-of-pack cementation and Chemical Vapor

Deposition (CVD) are also used for producing Pt-Al coatings [57]. A schematic of the equipment used for platinum plating is shown in Fig. 8. Usually, the pure platinum sheet with a thickness of 1 mm is the anode, and the specimen as the cathode is used. Also, the Direct current power supply with 0-10 A and 0-25 v is used, generally.

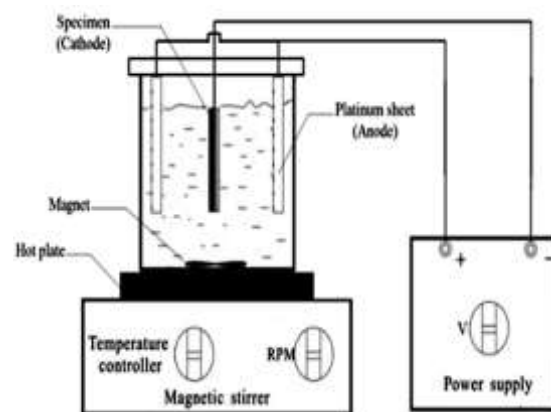


Fig. 8. Schematic of the equipment used for platinum electroplating.

There are three common types of electrolytes in industrial applications used for platinum electroplating:

**a: Hexa-chloro-platinic acid-based ( $\text{H}_2\text{PtCl}_6$ ):** Hexachloro-platinic acid can be used as a source of platinum. These will often utilize a phosphate buffer solution or can be based around an acid chloride-type bath. The processes exhibit high cathode efficiency and usually produce a bright deposit with relatively low stress. Deposits of up to 25  $\mu\text{m}$  have been produced successfully. The presence of chloride has limited their use in turbine applications as concerns related to corrosion are usually associated with chloride-containing electrolytes. Further, these electrolytes often use phosphate buffer systems that could be a concern in co-depositing residual traces of phosphorus in the platinum-aluminized layer. High cathode efficiency often, by default, leads to poor thickness distribution profiles with significant build-up on high current density areas.

**b: Platinum "Q" salt-based  $[(\text{NH}_3)_4\text{Pt}(\text{HPO}_4)]$ :** "Q" salt baths do not contain sulfur nor chlorine, but usually would contain some phosphorus within the complex of the "Q" salt itself  $[(\text{NH}_3)_4\text{Pt}(\text{HPO}_4)]$ . The "Q" Salt baths are usually operated at  $[\text{Pt}] = 5$  g/L,  $\text{pH} = 10.3$ , current density = 0.2-0.7  $\text{A}\cdot\text{dm}^{-2}$ , and temperature = 92  $^{\circ}\text{C}$ . The pH is adjusted with sodium hydroxide, which eliminates any need for ammonia. Operating at high temperature leads to high evaporation loss and regular addition of de-ionized or distilled water is

necessary in order to maintain the volume of the bath. Maintaining high temperature is critical, because the cathode current efficiency is substantially reduced at temperatures below 89 °C.

**c: “P” salt-based [(NH<sub>3</sub>)<sub>2</sub>Pt(NO<sub>2</sub>)<sub>2</sub>]:** “P” salt baths are very popular and are usually based on a solution matrix of mixed phosphates. Nitrite is often used as a processing stabilizer to help prevent the “P” salt transition from di-amine to tri-amine to tetra-amine. Formation of the tetra-amine is undesirable as, being a very stable complex; it tends to reduce the overall cathode efficiency of the plating bath. Nitrite, however, is in itself an unstable material, particularly at elevated temperatures. Nitrite-to-nitrate oxidation can easily take place but has the benefit of helping to facilitate platinum reduction. “P” salt baths are well established in turbine applications and appear to be well suited to the pack cementation process. They have as a result found significant applications in aircraft turbine blade production.

The baths usually do not contain any chlorine or sulfur, but will often use a phosphate-based conducting salt. The platinum “P” salt itself [(NH<sub>3</sub>)<sub>2</sub>Pt(NO<sub>2</sub>)<sub>2</sub>] does not contain any phosphorus as compared to the “Q” salt [(NH<sub>3</sub>)<sub>4</sub>Pt(HPO<sub>4</sub>)], which contains a phosphate functional group [58, 59].

#### 4.1. Microstructure of Pt-Aluminide Coatings

The range of microstructures that can be produced in Pt-Al coatings depends primarily on the processing conditions used, namely the temperature-time schedule of the prior diffusion and post aluminizing treatments, and the type of aluminizing process, and it is divided into three categories [58]:

##### 4.1.1. Inward Grown $\beta$ -(Ni,Pt)Al Coatings

The microstructure of Pt-Al coatings is shown in Fig. 9. Inward grown Pt-Al coatings exhibit a three-layer microstructure consisting of an outer Pt-rich layer, an intermediate layer and the inner IDZ.

The intermediate layer usually consists of  $\beta$ -NiAl phase and may contain some fine precipitates. A certain amount of Pt also remains in solid solution in the  $\beta$ -NiAl phase [35, 36, 61]. The IDZ has a precipitate-rich structure, as typically found in most diffusion aluminide coatings [9, 10, 61]. Depending on the processing conditions adopted, different microstructures for the outer Pt-rich layer can be achieved [15-17, 19]. The outer layer can be single-phase  $\xi$ -PtAl<sub>2</sub>, single-phase  $\beta$ -(Ni, Pt)Al, or a mixture of these two phases [44, 47, 62-65].

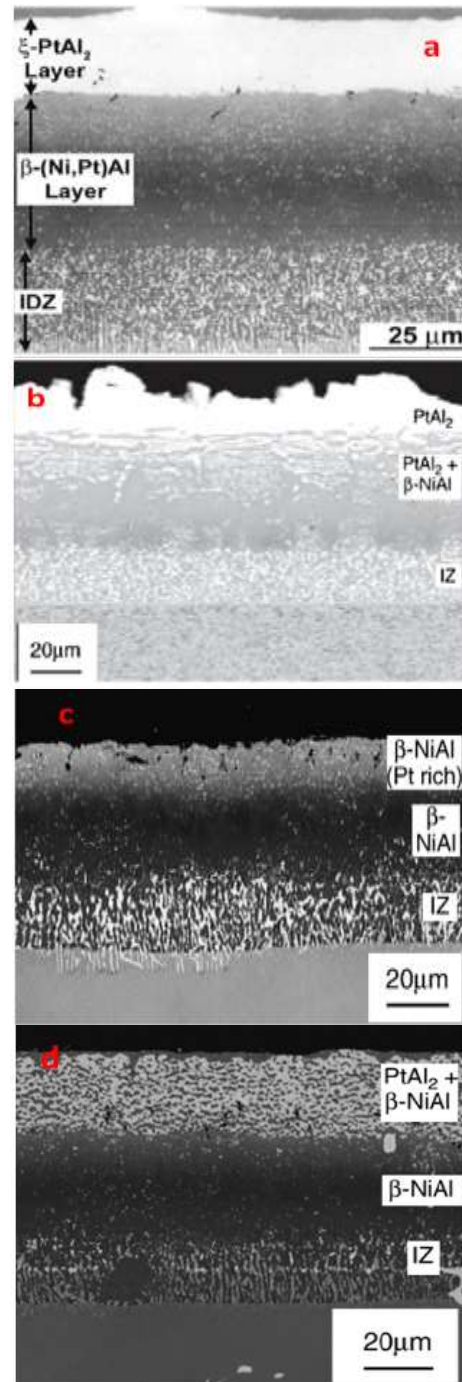


**Fig. 9. Schematic of various microstructures observed in an inward grown Pt-Al coating: (a) One limiting microstructure with the outer layer constituted of single-phase  $\xi$ -PtAl<sub>2</sub>, and the intermediate layer constituted of single-phase  $\beta$ -(Ni,Pt)Al, (b) One limiting microstructure with the outer layer constituted of single-phase  $\xi$ -PtAl<sub>2</sub>, and the intermediate layer constituted of dual-phase  $\beta$ -(Ni,Pt)Al +  $\xi$ -PtAl<sub>2</sub>, (c) One limiting microstructure with the outer layer showing a single phase  $\beta$ -NiAl structure in which the entire amount of Pt remains in solid solution and , (d) The other coating microstructure with the outer layer showing a dual-phase  $\beta$ -NiAl +  $\xi$ -PtAl<sub>2</sub>, and the intermediate layer constituted of single-phase  $\beta$ -(Ni,Pt)Al [62, 69, 70].**



The concentration of diffused platinum on the surface depends on the thickness of the electroplated platinum layer, the temperature, and the duration of the diffusion process.

If the Aluminum content in the aluminizing process is considered constant, then by increasing the concentration of platinum, it will be possible to form an outer layer including two  $\beta$  and  $\xi$  phases [44, 62, 63]. In addition to platinum, the concentration of aluminum also affects the microstructure of the coating to a lesser extent. By increasing the amount of diffused aluminum, it is possible to change the composition of the outer layer of the coat and increase its thickness. By increasing the aluminum content in the coating to a critical level, the microstructure of the coating remains unchanged, but its thickness continues to increase [66].

#### 4.1.2. Outward grown $\beta$ -(Ni,Pt)Al coatings

The typical microstructure of outward grown  $\beta$ -(Ni,Pt)Al coatings is similar to that obtained in case of low activity plain aluminide coatings [10]. They have a two-layer structure [36, 67].

The outer layer of the coating is constituted of single-phase  $\beta$ -(Ni,Pt)Al and the inner layer is the IDZ typically found in all aluminide coatings. Unlike the inward grown coatings, the outer layer of the outward coating contains virtually no precipitates.

These coatings are obtained under the rapid upward diffusion of nickel at high temperatures and low amounts of aluminum. Out-of-pack cementation and CVD methods are usually used to produce these types of coatings. An example of the two-layer microstructure of LAHT coatings is shown in Fig. 10. As can be seen, the outer layer of this coating consists of single phase  $\beta$ -(Ni, Pt)Al and has IDZ [68].

#### 4.1.3. Pt-Modified $\gamma$ - $\gamma'$ Coatings

HALT and LAHT coatings have disadvantages, which include: the formation of detrimental Topologically Closed Packed (TCP) phases of refractory elements in the substrate during heat treatment or service conditions, the formation of Substrate Diffusion Zone (SDZ) under the coating, the creation of  $\beta$ -phase aluminum concentration gradient from coating to the substrate and as a result of reducing its protective properties, producing stresses caused by the difference in thermal expansion coefficients of the coating and the substrate. The above disadvantages made  $\gamma$ - $\gamma'$  coatings to be more widely used.

These coatings have good chemical and mechanical compatibility with the substrate and have good oxidation resistance [60]. The coating shows a two-layer structure, somewhat similar to that of an outward grown  $\beta$ -(Ni,Al)Pt coating. However, unlike the  $\beta$  coating, the outer layer of a  $\gamma$ - $\gamma'$  coating consists primarily of  $\gamma'$  phase and the inner layer (IDZ) of  $\gamma$  and  $\gamma'$  phases, as shown in Fig. 11. Much fewer precipitates are present in the IDZ of a  $\gamma$ - $\gamma'$  coating as compared to HALT and LAHT coatings. The precipitates form mainly in the  $\gamma'$  phase of IDZ because of the relatively lower solubility of refractory elements in this phase as compared that in  $\gamma$  phase. Further, since the solubility is higher in  $\gamma'$  than in  $\beta$ -NiAl, a lower volume fraction of precipitates forms in the IDZ of the  $\gamma$ - $\gamma'$  coating as compared to the HALT and LAHT coatings [73]. For the formation of this coating, the amount of diffused aluminum should be very low.

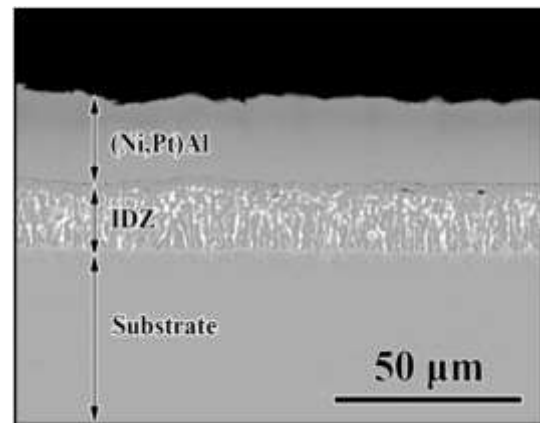


Fig. 10. The typical microstructure of an outward grown Pt-Al coating [71].

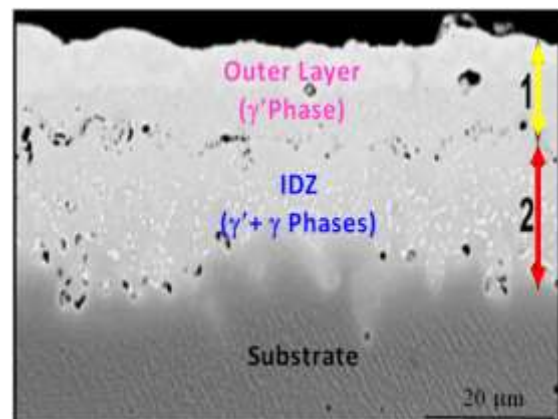


Fig. 11. The typical microstructure of a Pt-modified  $\gamma$ - $\gamma'$  coating deposited on a Ni-base superalloy [72]. The numbers 1 and 2 indicate the outer layer and the IDZ of the coating.

#### 4.2. Role of Pt in Enhancing Oxidation and Hot Corrosion Resistance

It has long been known that the presence of Pt in superalloys and in aluminide coatings leads to considerable improvements in high temperature oxidation and hot corrosion resistance [61, 74-78]. The mechanisms that lead to the improvement of oxidation and hot corrosion resistance of Pt-Al coatings are:

##### a) Improving adhesion of protective $\alpha$ -Al<sub>2</sub>O<sub>3</sub> to the substrate:

Pt is believed to reduce the stresses in the scale and, thereby, improve the scale adhesion. It has been conjectured that such reduction in the growth stresses in the oxide scale is achieved through the incorporation of Pt in the scale in the form of volatile PtO<sub>2</sub> at the oxidation temperature [76, 78-80].

It has also been suggested that Pt enhances the oxide scale adhesion to the coated substrate by promoting the formation of Al<sub>2</sub>O<sub>3</sub> pegs that grow into the substrate [81, 82]. These pegs are believed to keep the scale anchored to the coated substrate. Pint et al. [83] determined the diffusion of aluminum into the metal substrate, the segregation of elements at the interface of  $\alpha$ -Al<sub>2</sub>O<sub>3</sub>/substrate and grain boundaries of  $\alpha$ -Al<sub>2</sub>O<sub>3</sub> and the generation of stress in  $\alpha$ -Al<sub>2</sub>O<sub>3</sub> as the most important factors in reducing the adhesion of the oxide scale.

##### b) Increasing the contact area between TGO and BC:

Svensson et al. [84] have concluded that the beneficial effect of Pt on scale adhesion is due to the enhancement of contact area between the TGO layer and the metallic coating. This is achieved because Pt helps reduce the formation of interfacial voids [78, 85] and also promotes filling of the created cavities with the oxide. As a result, the contact areas between the oxide and the metal increases which raises the effective work needed to separate the scale from the metal [51].

Carling and Carter [86] determined that platinum does not directly increase the adhesion of alumina to the  $\beta$ -NiAl phase and the mechanism of platinum's effect on the growth rate of the  $\alpha$ -Al<sub>2</sub>O<sub>3</sub> layer is different from the effect of active elements such as yttrium, zinc, and hafnium. These elements reduce the outward diffusion rate of Al<sup>3+</sup> and slow down the formation of TGO [87, 88]. For example, Zr along with Al is placed at the IDZ/ $\beta$ -NiAl interface. Then, during oxidation, it migrates to the boundaries of  $\beta$ -NiAl through upward diffusion and reduces cavitation in the grain boundaries.

Tan et al. [89] have shown that the finer the TGO is, the better its adhesion to BC which increases the

strength of the TGO/BC interface and prevents the formation of micro-voids in the interface.

##### c) Increasing the diffusivity of aluminum in the $\beta$ -NiAl phase:

Platinum decreases the formation energies of point defects and defect clusters in the  $\beta$ -NiAl phase which leads to the enhancement in the diffusivity of Al in  $\beta$ -NiAl [90]. Kiruthika et al. [91] stated that platinum is substituted in the atomic structure of nickel.

By increasing the platinum content the point defect formation energy as well as the migration energy of atoms in the  $\beta$  phase decreases, and the diffusion rate of platinum increases. By comparing the adsorption energies of platinum with  $\alpha$ -Al<sub>2</sub>O<sub>3</sub> and  $\beta$ -NiAl, Hinnemann and Carter [92] concluded that platinum has a greater tendency to associate with  $\beta$ -NiAl and has an effect on its diffusivity. Meanwhile, Svensson et al. [93] and Prescott et al. [94] determined that if the concentration of platinum in the coating is appropriate, the probability of forming a continuous and stable layer of  $\alpha$ -Al<sub>2</sub>O<sub>3</sub> instead of unstable phases  $\theta$ -Al<sub>2</sub>O<sub>3</sub> and  $\gamma$ -Al<sub>2</sub>O<sub>3</sub> will be higher. During the service of aluminide coatings at high temperatures, aluminum continuously diffuses from BC to the BC/TC interface and forms the TGO layer. Therefore, the aluminum concentration in the BC/TC interface is reduced and the formation of brittle oxides is possible. In addition, refractory elements diffuse from the substrate to the coating and spinel phases are formed at the BC/TC interface.

During oxidation, platinum prevents the formation of spinel compounds, reducing the diffusion rate of the substrate alloy elements into the coating and increasing the diffusion rate of aluminum into the BC/TC interface [11, 95-97].

##### d) Preventing the segregation of sulfur at the TGO/BC interface

Pt is believed to inhibit the segregation of S to alumina scale/coating interface and, thereby, enhances the scale adhesion to the coating. Platinum reduces the formation of micro-voids caused by cyclic oxidation at the oxide scale/substrate interface. Micro-voids are suitable sites for segregating sulfur and coating impurities such as chlorine and phosphorus, which causes a reduction in coating strength [98-101].

Zhang et al. [102, 103] showed the effect of platinum on increasing the adhesion of the TGO layer during cyclic oxidation and also reducing the formation of micro-voids at the oxide scale/substrate interface even in the presence of high sulfur content in the coating.

#### e) Reducing the $\beta$ -NiAl to $\gamma'$ -Ni<sub>3</sub>Al phase transformation rate:

Pt improves the oxidation resistance of the coating because of its ability to lower the transformation rate of  $\beta$ -(Ni,Pt)Al phase of the coating to less Al-rich phases such as  $\gamma'$ -Ni<sub>3</sub>Al [54], to inhibit the formation of  $\alpha$ -Cr and  $\alpha$ -W precipitates in the coating [104] and to increase the coating stability against inward diffusion of Al and/or outward diffusion of Ni and refractory elements such as Mo, V and W [68, 104]. Swadzba et al. [43] stated that the reversible transformation of  $\beta$ -(Ni,Pt)Al or  $\beta$ -NiAl to  $\gamma'$ -Ni<sub>3</sub>Al causes detrimental thermal strains due to mismatch of thermal expansion coefficients between the substrate and the TC layer.

#### 4.3. The effect of prior treatment on the microstructure of Pt-aluminide coating

Diffusion annealing heat treatment before applying TBC coating affects the TGO density formed during thermal cycles [105].

If annealing is not performed, platinum separates from the surface due to the mismatch in thermal expansion coefficient with the substrate [52, 62, 106]. If the thickness of the platinum electroplating layer increases, the surface roughness decreases. Chen et al. [107] stated that after the annealing, the IDZ zone and the roughness of the coating surface increase due to the difference in the inter-diffusion rate of platinum and nickel. Also, volumetric strains increase, and the fracture toughness of the coating decrease due to the difference in the atomic radius of nickel and platinum [108]. Yavorska et al. [109] have investigated the effect of annealing heat treatment after platinum electroplating. They confirmed that the thickness of the electroplated platinum layer, the inward diffusion of platinum, and the outward diffusion of nickel and chromium increased during the annealing. Therefore, the formation of  $\beta$ -(Ni, Pt)Al phase in the aluminizing is facilitated. The  $\beta$ -(Ni, Pt)Al phase transforms to Ni<sub>3</sub>Al much slower than the  $\beta$ -NiAl phase and also facilitates the growth of Al<sub>2</sub>O<sub>3</sub> [110].

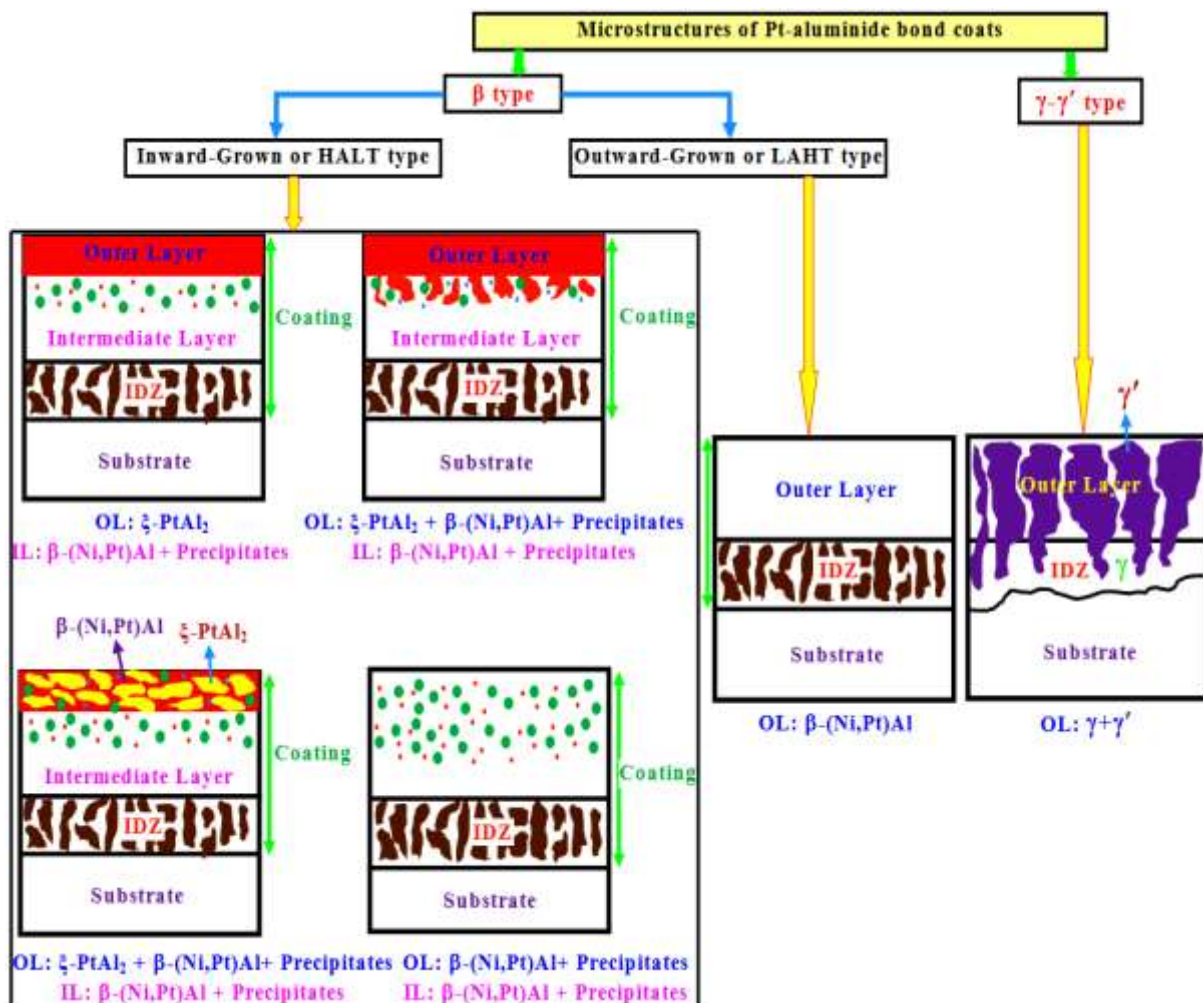


Fig. 12. Schematic illustration of the entire gamut of microstructures observed in case of Pt-modified aluminide coatings on Ni-base superalloys. The phases present in outer layer (OL) and intermediate layer (IL) of the coatings have been mentioned.

Benoist et al. [63] found that the annealing heat treatment of platinum causes the formation of a dual-phase structure that includes PtAl<sub>2</sub> particles in a NiAl matrix. Otherwise, PtAl<sub>2</sub> will be formed as a continuous layer on the coating surface. If the thickness of the electroplated platinum layer increases, then the amount of PtAl<sub>2</sub> phase in the coating increases [111]. PtAl<sub>2</sub> has the highest hot corrosion resistance but the least ductility [106].

The parameters affecting the microstructure of platinum-aluminide coatings are the thickness of the electroplated platinum layer, the diffusion annealing of the platinum layer, the surface roughness of the substrate, the chemical composition of the substrate, the temperature and the aluminizing process [46]. If the thickness of the platinum plating layer is 2-8 μm, the final Pt-Al coating will have the highest surface roughness [108]. Through surface treatments such as sand-blasting, the surface roughness of Pt-Al coatings and the thickness of the TGO layer decrease, and the oxidation resistance of the BC coating increases [112]. Lee et al. [113] and Zhou et al. [20] confirmed the role of surface roughness in increasing the cyclic oxidation and hot corrosion resistance of Pt-Al coatings and stated that platinum stabilizes the β-(Ni, Pt)Al phase and prevents Aluminum depletion in the TGO layer. The entire gamut of microstructures observed in Pt-Al bond coats have been schematically summarized in Fig. 12.

#### 4. Conclusion

In the present review, an attempt has been made to collate the reported information on the microstructural aspects of TBCs with different Pt-modified aluminide bond coats, including β-(Ni, Pt)Al and γ-γ' coatings, on Ni-base superalloys.

TBCs are a surface protection technology by applying ceramic on a metal substrate like gas turbine blades/vanes, which can increase operation temperature, high-temperature corrosion resistance, and the lifetime of the metal hot section with the consequence of increasing the efficiency of turbine engines. A TBC should have low thermal conductivity, high melting point, chemically inert at high temperatures, high-temperature phase stability, coefficients of thermal expansion close to the metal substrate, and resistance to sintering to maintain the pores present in the coating. A typical TBC system consists of three layers, a ceramic top coat (TC), generally, Ytria stabilized zirconia (YSZ) playing an insulating role, an aluminum-rich reservoir such as an MCrAlY (M = Ni, Co or Ni, and Co) or a platinum-aluminide (Pt-Al) metallic bond coat (BC), increasing the antioxidant capacity

of the metallic substrate and elevating the bond strength between ceramic and substrate, and a thermally grown oxide layer (TGO), which is a high-temperature oxidation product. Each layer possesses different thermal-physical properties being temperature-dependent, which together control the lifetime of the coating.

Electron-beam physical vapor deposition (EB-PVD) and atmospheric plasma spraying (APS) are two commonly used methods for preparing TBCs in industry.

APS process is highly cost-effective and has a wide range of spray materials compared with EB-PVD. While the coatings produced by EB-PVD have a columnar structure and are comparatively much more strain-tolerant. In addition, TBCs prepared by APS generally have a lower thermal conductivity than that of EB-PVD coatings. The APS coating exhibits typical lamellar structure characteristics with a series of splats stacked up with each other. The defects in APS coating resulting from the spraying process can be fallen into three categories: (i) large porosities, which is due to the incomplete fulfillment between depositing splats or semi-molten powders, (ii) lateral porosities between lamellae, referred to as inter-splat crack, (iii) vertical porosities at the periphery of splats, namely intra-splat crack. Apart from various pores, a power of un-molten particles also appears within the coating. These defects affect thermal conductivity and are preferable failure initiation sites.

β-(Ni, Pt)Al and γ-γ' bond coats are formed by depositing a layer of Pt on the superalloy substrate by electroplating and subjecting the plated specimen to a diffusion treatment in a vacuum. Subsequently, the specimen is aluminized and given a post-aluminizing heat treatment to complete coating formation. Pt-aluminide coatings are produced by pack cementation or chemical vapor deposition (CVD). Pack cementation applies to external surfaces. While CVD is an effective method and the prepared coating can cover the whole component including the internal surfaces. The Al concentration of the coating is varied by altering the activity of Al in the aluminizing medium, which in turn is controlled by the time-temperature schedule of the aluminizing treatment and/or the amount of Al present in the aluminizing medium.

Among the β bond coats, depending on the growth mechanism during aluminizing treatment, the coating is either called inward-grown or outward-grown. The inward-grown or high-activity β coatings typically have a three-layer structure consisting of a Pt-rich outer, an intermediate layer, and an inner inter-diffusion zone (IDZ). The Pt-rich outer layer can have a single-phase ξ-PtAl<sub>2</sub> or a two-phase ξ-PtAl<sub>2</sub> + β-(Ni, Pt)Al or a single-phase β-(Ni, Pt)Al structure depending on the Pt and Al concentrations in the layer, as summarized in Fig.

12. The outward grown or low activity  $\beta$  bond coats always have a two-layer structure in which the outer layer consists of single-phase  $\beta$  and the inner layer is the IDZ. The outward-grown coatings contain significantly lower Al than their inward-grown counterparts. Unlike the  $\beta$  bond coats, the  $\gamma$ - $\gamma'$  coatings always have a  $\gamma + \gamma'$  structure.

Various investigations indicate that the addition of Pt to NiAl coatings has the beneficial following effects on their high-temperature oxidation and hot corrosion resistance: (a) Inducing peg formation in the scale which results in its improved anchoring to the coated substrate; (b) enhancing the scale adhesion by reducing the segregation of harmful elements such as Sulfur to the scale/coating interface and/or by reducing void formation at the interface; (c) Promoting the diffusion and selective oxidation of Al to form pure oxides; (d) Inhibiting the external diffusion of refractory elements from the substrate to the coating; (e) Increasing the surface roughness of TGO due to excessive Pt.

For commercial use, only Pt-modified  $\beta$  bond coats, especially the low activity or outward-grown variety, are currently being used. Some of the commercially available Pt-Al bond coats are RT22, SS82A and MDC150L. RT22 and SS82A are inward-grown (high activity) coatings while MDC150L is an outward-grown (low activity) coating.

## References

- [1] R. C. Reed: *The Superalloys-Fundamentals and Applications*, Cambridge University Press, New York, (2006), 261
- [2] P. Lindloff: *Space Engineering: Structural Materials Handbook- Part 5: New Advanced Materials*, Advanced Metallic Materials, General Design Aspects and Load Transfer and Design of Joints, ESA Requirements & Standards Division, ESTEC, Noordwijk, (2011), 58.
- [3] D. Francois, A. Pineau and A. Zaoui: *Mechanical Behaviour of Materials-Solid Mechanics and Its Application*. Chapter 8: Creep-Fatigue-Oxidation Interaction, Springer, Dordrecht, (2013), 407.
- [4] D. J. Leo, M. J. Walsh, D. Mclashlan, and A. M. Kursunsky, *Int. J. Fatigue*, 31(2009), 1966.
- [5] T. K. Kim, J. Yu and J. Y. Jeon, *Metall. Mater. Trans. A*, 23A(1992), 2581.
- [6] R. W. Fawley: *The Superalloys*, Wiley, New York, (1972), 312.
- [7] I. Gurrappa, I. V. S. Yashwanth and I. Mounika: *Gas Turbines - Materials, Modeling and Performance*, Chapter 3: The Importance of Hot, Corrosion and its Effective Prevention for Enhanced Efficiency of Gas Turbines, INTECH Publication, New York, (2015), 55.
- [8] D. Driver, D. W. Hall, and G. W. Meetham: *The Gas Turbine Engine, the Development of Gas Turbine Materials*, Springer, London, (1981), 175.
- [9] U. Schulz, K. Fritscher, C. Leyens, M. Peters and W. A. Kaysser, *JOM*, 49(1997), 370.
- [10] M. Góral, P. Sosnowy, J. Achiev. *Mater. Manuf. Eng.*, 55(2012), 912.
- [11] K.A. Marino, E.A. Carter, *Acta Mater.* , 58(2010), 2726.
- [12] M. Góral, M. Pytel, W. Cmela and M. Drajewicz, *Solid State Phenom.* , 227(2015), 321.
- [13] D. R. Clarke, M. Oechsner and N.P. Padture, *MRS Bull.*, 37(2012), 891.
- [14] A. Afrasiabi, M. Saremi and A. Kobayashi, *Mater. Sci. Eng. A*, 478(2008), 264.
- [15] X. Chen, Y. Zhao, L. Gu, B. Zou, Y. Wang and X. Cao, *Corros. Sci.*, 53(2011), 2335.
- [16] X. Chen, Y. Zhao, X. Fan, Y. Liu, B. Zou, Y. Wang, H. Ma and X. Cao, *Surf. Coat. Technol.*, 205(2011), 3293.
- [17] Y. Wang and G. Sayre, *Surf. Coat. Technol.*, 203(2009), 2186.
- [18] D. R. Clarke, *Surf. Coat. Technol.*, 163 (2003), 67.
- [19] Y. He, K. N. Lee, S. Tewari and R. A Miller, *J. Therm. Spray Technol.*, 9(2000), 59.
- [20] D. Zhou, O. Guillon and R. Vaßen, *Coatings*, 7(2017), 1.
- [21] V. Postolenko, *Failure mechanisms of thermal barrier coatings for high temperature gas turbine components under cyclic thermal loading*, Ph.D Thesis, Kiev University, Kiev, Ukraine (2008).
- [22] H. Zhao, *Low conductivity thermal barrier coatings*, Ph.D Thesis, the School of Engineering and Applied Science, University of Virginia, Virginia, USA (2009).
- [23] T. M. Pollock, D. M. Lipkin and K. J. Hemker, *MRS Bull.*, 37(2012), 923.
- [24] A. Rabieifar, S. Nategh, M.R. Afshar and H. Najafi, *Mater. Res. Express*, 7(2020), 1.
- [25] Q. Hongyu, Y. Xiaoguang and W. Yamei, *Int J Fract.* , 157(2009), 71.
- [26] J. R. Nicholls, N. J. Simms, W. Chan and H. E. Evans, *Surf. Coat. Technol.*, 149(2002), 236.
- [27] Z. G. Liu, J. H. Ouyang, Y. Zhou and X. L. Xia, *J. Eur. Ceram. Soc.*, 29(2009), 2423.
- [28] Y. Liu, T. Nakamura, V. Srinivasan, A. Vaidya, A. Gouldstone and S. Sampath, *Acta Mater.*, 55(2007), 4667.
- [29] S. Sampath, U. Schulz, M. O. Jarligo and S. Kurod, *MRS Bull.*, 37(2012), 903.
- [30] S. Kurod and T.W. Clyne, *Thin Solid Films*, 200(1991), 49.
- [31] D. D. Hass, *Thermal Barrier Coatings, Directed Vapor Deposition of Thermal Barrier Coatings*, Ph.D Thesis, the School of Engineering and Applied Science, University of Virginia, Virginia, USA (2000).
- [32] A. Kawasaki and R. Watanabe, *Mater. Sci. Forum*, 308-311(1999), 402.

- [33] A. Feuerstein, J. Knapp, T. Taylor, A. Ashary, A. Bolcavage and N. Hitchman, *J. Therm. Spray Technol.*, 17(2008), 199.
- [34] S. Bose: *High Temperature Coatings*, Elsevier, Amsterdam, (2007), 145.
- [35] U. Leushake, T. Krell, U. Schulz, M. Peters, W. A. Kaysser and B. H. Rabin, *Surf. Coat. Technol.*, 94(1997), 131.
- [36] A. Keyvani, M. Saremi and M.H. Sohi, *J. Alloys Compd.*, 506(2010), 103.
- [37] Z. Chen, N. Q. Wu, J. Singh and S. X. Mao, *Thin Solid Films*, 443(2003), 46.
- [38] H. Singh, S. S. Chatha, H. S. Sidhu and K. Sharma, *Int. J. Adv. Robot. Syst.*, 3(2011), 85.
- [39] Z. Zhan, Z. Liu, J. Liu, L. Li, Z. Li and P. Liao, *Appl. Surf. Sci.*, 256(2010), 3874.
- [40] J. Liu, H. J. Choi and Y. H. Sohn, 47th AIAA Aerospace Sciences Meeting Including the New Horizons Forum and Aerospace Exposition, American Institute of Aeronautics and Astronautics, Florida, (2009), 94.
- [41] K. Shirvani, M. Saremi, M. A. Nishikata and T. Tsuru, *Mater. Trans.*, 43(2002), 2622.
- [42] J. W. Lee and Y. C. Kuo, *Surf. Coat. Technol.*, 201(2006), 3867.
- [43] R. Swadzba, M. Hetmańczyk, J. Wiedermann, L. Swadzba, G. Moskal, B. Witala and K. Radwański, *Surf. Coat. Technol.*, 215(2013), 16.
- [44] N. Vialas and D. Monceau, *Surf. Coat. Technol.*, 201(2006), 3846.
- [45] R. E. Malush, P. Deaband and D.H. Boone, *Surf. Coat. Technol.*, 36(1988), 13.
- [46] B. A. Pint, J. A. Haynes and Y. Zhang, *Surf. Coat. Technol.*, 205(2010), 1236.
- [47] K. Shirvani, S. Firouzi and A. Rashidghamat, *Corros. Sci.*, 55(2012), 378.
- [48] R. Swadzba, J. Wiedermann, M. Hetmańczyk, L. Swadzba, B. Mendala, B. Witala and Ł. Komendera, *Surf. Coat. Technol.*, 237(2013), 16.
- [49] Y. Q. Wang and G. Sayre, *Surf. Coat. Technol.*, 203(2008), 256.
- [50] G. P. Cammarota, A. Casagrande and G. Sambogna, *Surf. Coat. Technol.*, 201(2006), 230.
- [51] C. T. Liu, J. Ma, X. F. Sun and P. C. Zhao, *Surf. Coat. Technol.*, 204(2010), 3641.
- [52] R. Streiff and D. H. Boone, *J. Mater. Eng.*, 10(1988), 15.
- [53] W. Goward and D. H. Boone, *Oxid. Met.*, 3(1971), 475.
- [54] G. Lehnert and H. Meinhardt, *Surf. Coat. Technol.*, 1(1972), 71.
- [55] G. C. Fryburg, F. J. Kohl and C. A. Stearns, *J. Electrochem. Soc.*, 131(1984), 2958.
- [56] M. R. Jackson and J. R. Rairden, *Metall Trans. A*, 8A(1977), 1697.
- [57] J. A. Conner, *Int. Gas Turbines and Aeroengines Congress and Exposition*, ASME, Cologne, (1992), 1.
- [58] R. L. Penven, W. Levason and D. Pletcher, *J. Appl. Electrochem.*, 22(1992), 415.
- [59] S. J. Hemsley and W. Zhou, *Trans. Inst. Met. Finish.*, 88(2010), 11.
- [60] D. K. Das, *Prog. Mater. Sci.*, 58(2013), 151.
- [61] G. W. Goward, *Surf. Coat. Technol.*, 108-109(1998), 73.
- [62] D. K. Das, V. Singh and S. V. Joshi, *Metall Mater. Trans. A*, 31A(2000), 2037.
- [63] J. Benoist, K. F. Badawi, A. Malie and C. Ramade, *Surf. Coat. Technol.*, 194(2005), 48.
- [64] F. Pedraza, A. Kennedy, J. Kopecek and P. Moretto, *Surf. Coat. Technol.*, 200(2006), 4032.
- [65] Y. Q. Wang and G. Sayre, *Surf. Coat. Technol.*, 203(2009), 1264.
- [66] D. K. Das, V. Singh and S. V. Joshi, *Oxid. Met.*, 57(2002), 245.
- [67] H. M. Tawancy and M. Al-Hadhrani, *J. Eng. Gas Turbine Power*, 134(2012), 012101.
- [68] J. Angenete and K. Stiller, *Surf. Coat. Technol.*, 150(2002), 107.
- [69] G. R. Krishna, D. K. Das, V. Singh and S. V. Joshi, *Mater. Sci. Eng. A*, 251(1998), 40.
- [70] D. K. Das and J. Annapurna, *Development of Pt-aluminide coatings on CM-247 Ni-base superalloy: A preliminary study on mechanism of coating formation*, Defence metallurgical research center, Hyderabad, (1996), 187.
- [71] Y. Li, S. Li, C. Zhang, N. Xu and Z. Bao, *Crystals*, 11(2021), 972.
- [72] D. K. Das, B. Gleeson, K. S. Murphy, S. Ma and T. M. Pollok, *Mater. Sci. Technol.*, 25(2009), 300.
- [73] P. Audigie, S. Selezneff, A. V. Put, C. Estourne, S. Hamadi and D. Monceau, *Oxid. Met.*, 81(2014), 33.
- [74] T. A. Kircher, B. G. Mc Mordieand and A. McCarter, *Surf. Coat. Technol.*, 68-69(1994), 32.
- [75] G. J. Tatlock, T. J. Hurd and J. S. Punni, *Platin Met. Rev.*, 31(1987), 26.
- [76] J. G. Fountain, F. A. Golightly, F. H. Scott and G. C. Wood, *Oxid. Met.*, 10(1976), 341.
- [77] D. J. Young: *High Temperature Oxidation and Corrosion of Metal*, Elsevier, Amsterdam, (2008), 214.
- [78] J. H. W. De Wit and P. A. Van Manen, *Mater. Sci. Forum.*, 154(1994), 109.
- [79] G. R. Johnston, J. L. Cocking and W. C. Johnson, *Oxid. Met.*, 23(1985), 237.
- [80] S. B. Newcomb, W. M. Stobbs, *Proc. Conf. on elevated temperature coatings: science and technology II*, Metals Mater. Soc. Anaheim, California, (1996), 265.
- [81] K. L. Luthra and H. S. Spacil, *J. Electrochem. Soc.*, 129(1982), 649.
- [82] I. M. Allam, H. C. Akuezue and D. P. Whittle, *Oxid. Met.*, 14(1980), 517.
- [83] B. A. Pint, I. G. Wright, W. Y. Lee, Y. Zhang, K. Prubner and K. B. Alexander, *Mater. Sci. Eng. A*, 245(1998), 201.

- [84] H. Svensson, M. Christensen, P. Knutsson, G. Wahnström and K. Stiller, *Corros. Sci.*, 51(2009), 539.
- [85] N. Birks, G. H. Meier and F. S. Petit: *Introduction to the High Temperature Oxidation of Metals*, Cambridge University Press, New York, (2006), 275.
- [86] K. M. Carling, E. A. Carter, *Acta Mater.*, 55(2007), 2791.
- [87] A. H. Heuer and D. B. Hovis, *J. Am. Ceram. Soc.*, 94(2011), 146.
- [88] B. A. Pint, *Oxid Met.*, 45(1996), 1.
- [89] X. Tan, X. Peng and F. Wang, *Corros. Sci.*, 85(2014), 280.
- [90] K. A. Marino and E. A. Carter, *Acta Mater.*, 56(2008), 3502.
- [91] P. Kiruthika and A. Paul, *Philos. Mag. Lett.*, 95(2015), 138.
- [92] B. Hinnemann and E. A. Carter, *J. Phys. Chem.*, 111(2007), 7105.
- [93] H. Svensson, J. Angenete and K. Stiller, *Surf. Coat. Technol.*, 177-178(2004), 152.
- [94] R. Prescott and M. J. Graham, *Oxid Met.*, 38(1992), 233.
- [95] C. Leyens, B. A. Pint and I. G. Wright, *Surf. Coat. Technol.*, 133(2000), 15.
- [96] D. Liu, P. E. Flewitt and M. Pavier, *Procedia Manuf.*, 3(2014), 1729.
- [97] B. A. Pint, *Surf. Coat. Technol.*, 188-189(2004), 71.
- [98] J. A. Haynes, K. L. More, B. A. Pint, I. G. Wright, K. Cooley and Y. Zhang, *Mater. Sci. Forum*, 369-372(2001), 679.
- [99] P. Y. Hou and V. K. Tolpygo, *Surf. Coat. Technol.*, 202(2007), 623.
- [100] B. A. Pint and K. L. More, *J. Mater. Sci.*, 44(2009), 1676.
- [101] K. A. Unocic, C. M. Parish and B. A. Pint, *Surf. Coat. Technol.*, 206(2011), 1522.
- [102] Y. Zhang, W. Y. Lee, J. A. Haynes, I. G. Wright, B. A. Pint, K. M. Cooley and P. K. Liaw, *Metall. Mater. Trans. A*, 30A(1999), 2679.
- [103] Y. Zhang, J.A. Haynes, W.Y. Lee, I.G. Wright, B.A. Pint, K.M. Cooley and P.K. Liaw, *Metall. Mater. Trans. A*, 32A(2001), 1727.
- [104] N. Otsuka and R.A. Rapp, *J. Electrochem. Soc.*, 137(1990), 46.
- [105] B. Baufeld and U. Schulz, *Surf. Coat. Technol.*, 201(2006), 2667.
- [106] Y. Tamarin: *Protective Coatings for Turbine Blades*, ASM Int., Ohio, (2002), 55.
- [107] S. Chen, F. Ke, M. Zhou and Y. Bai, *Acta Mater.*, 55(2007), 3169.
- [108] S. J. Hong, G. H. Hwang, W. K. Han and S. G. Kang, *Surf. Coat. Technol.*, 203(2009), 3066.
- [109] M. Yavorska and J. Sieniawski, *Arch. Mater. Sci. Eng.*, 45(2010), 56.
- [110] J. Benoist, K. F. Badawi, A. Malie and C. Ramade, *Surf. Coat. Technol.*, 182(2004), 14.
- [111] K. G. S. Thomas and M. Hertter, *Surf. Coat. Technol.*, 120-121(1999), 84.
- [112] A. C. Karaoglanli, K. M. Doleker, B. Demirel, A. Turk and R. Varol, *Appl. Surf. Sci.*, 354(2015), 314.
- [113] J. H. Lee, P. C. Tsai and J. W. Lee, *Thin Solid Films*, 517(2009), 5253.